© 2014. Published by The Company of Biologists Ltd | Journal of Cell Science (2014) 127, 1104–1116 doi:10.1242/jcs.143743

RESEARCH ARTICLE

Vinculin directly binds zonula occludens-1 and is essential for stabilizing connexin-43-containing gap junctions in cardiac myocytes

Alice E. Zemljic-Harpf[1,2], Joseph C. Godoy[1,3], Oleksandr Platoshyn[2], Elizabeth K. Asfaw[1,3], Anna R. Busija[2], Andrea A. Domenighetti[3] and Robert S. Ross[1,3,*]

ABSTRACT

Vinculin (Vcl) links actin filaments to integrin- and cadherin-based cellular junctions. Zonula occludens-1 (ZO-1, also known as TJP1) binds connexin-43 (Cx43, also known as GJA1), cadherin and actin. Vcl and ZO-1 anchor the actin cytoskeleton to the sarcolemma. Given that loss of Vcl from cardiomyocytes causes maldistribution of Cx43 and predisposes cardiomyocyte-specific Vcl-knockout mice with preserved heart function to arrhythmia and sudden death, we hypothesized that Vcl and ZO-1 interact and that loss of this interaction destabilizes gap junctions. We found that Vcl, Cx43 and ZO-1 colocalized at the intercalated disc. Loss of cardiomyocyte Vcl caused parallel loss of ZO-1 from intercalated dics. Vcl co-immunoprecipitated Cx43 and ZO-1, and directly bound ZO-1 in yeast two-hybrid studies. Excision of the *Vcl* gene in neonatal mouse cardiomyocytes caused a reduction in the amount of Vcl mRNA transcript and protein expression leading to (1) decreased protein expression of Cx43, ZO-1, talin, and β1D-integrin, (2) reduced PI3K activation, (3) increased activation of Akt, Erk1 and Erk2, and (4) cardiomyocyte necrosis. In summary, this is the first study showing a direct interaction between Vcl and ZO-1 and illustrates how Vcl plays a crucial role in stabilizing gap junctions and myocyte integrity.

KEY WORDS: Cardiac myocyte, Gap junction, Vinculin, Vcl, Zonula occludens-1, ZO-1, Heart

INTRODUCTION

With continual cycles of contraction and relaxation, cardiac myocytes are normally under significant mechanical stress. Thus, it is essential that a strong anchorage between cardiac myocytes, the extracellular matrix and other cells be adequately maintained. If anchorage is impaired, membrane instability might result, leading to pathological remodeling and heart failure (Kostin et al., 2000; Tirziu et al., 2010).

Vinculin (Vcl) is an actin-binding and membrane-associated protein found in both cell–matrix and cell–cell junctions. When bound to ligands, such as acidic phospholipids (Gilmore and Burridge, 1996; Weekes et al., 1996), talin (Izard et al., 2004) and α-actinin (Bois et al., 2006), intramolecular bonds are unmasked, thereby initiating Vcl activation (Ziegler et al., 2006). One of unique features of Vcl is to anchor and to assemble the actin cytoskeleton to the cell membrane through either integrin-containing focal adhesions or cadherin/catenin-containing adherens junctions (Grashoff et al., 2010; Hu et al., 2007). Izard's group has determined the crystal structure of full-length human Vcl, and described the assembly of a globular head, hinge region and flexible tail (Borgon et al., 2004).

Vcl is known to insert into the acidic-phospholipid-containing bilayer (Niggli et al., 1986; Niggli and Gimona, 1993). Phosphatidylinositides are integral phospholipids positioned at the cytosolic side of eukaryotic cell membranes. They are important for organizing the membrane–cytosol interface, as well as signal transduction (Di Paolo and De Camilli, 2006). The acidic phospholipid phosphatidylinositol (4,5)-bisphosphate [PtdIns(4,5)P_2, PIP_2] directly regulates the actin cytoskeleton by modulating the activity and targeting of actin regulatory proteins (Yin and Janmey, 2003). Vcl binds PIP_2, thereby acting as a sensor that can modify how phospholipids regulate the coupling of adhesion sites to the actin cytoskeleton (Chandrasekar et al., 2005; Palmer et al., 2009). Class I phosphoinositide 3-kinases (PI3Ks) phosphorylate phospholipids including PIP_2, and act as scaffolding adapters (Costa and Hirsch, 2010). Hence, PI3Ks can generate phosphatidylinositol (3,4,5)-triphosphate [PtdIns(3,4,5)P_3, PIP_3], which plays numerous roles in many cells, including key functions in cardiac myocyte cell survival (Ghigo et al., 2012). PIP_2-activated Vcl recruits focal adhesion proteins, such as actin and talin, to integrin-containing cell adhesion sites (Gilmore and Burridge, 1996). However, how altered Vcl protein expression might affect PI3K activation is currently unclear.

The zonula occludens (ZO) family consists of ZO-1, -2 and -3 proteins (also known as TPJ1, TJP2 and TJP3, respectively). They are present in tight junctions and adherens junctions, as well as gap junctions (Inoko et al., 2003; Jesaitis and Goodenough, 1994). ZO proteins bind a large number of partners including connexin (Cx) proteins and α-actinin, α-catenin, occludin, claudin, shroom-2, nephrin, F-actin and afadin, highlighting their role as important cytosolic scaffolding proteins (Fanning and Anderson, 2009; Fanning et al., 2002). In cardiac myocytes, the second PDZ domain of ZO-1 directly interacts with the gap junctional protein Cx43 (also known as GJA1) (Giepmans and Moolenaar, 1998; Toyofuku et al., 1998). Global deletion of the ZO-1 gene in the mouse results in delayed growth and development from E8.5 onward, with both embryonic and extra-embryonic defects evident, including abnormal angiogenesis. This leads to embryonic lethality by E11.5 (Katsuno et al., 2008).

[1]Veterans Administration Healthcare San Diego, San Diego, CA 92161, USA. [2]University of California, San Diego School of Medicine, Department of Anesthesiology, La Jolla, CA 92093, USA. [3]University of California, San Diego School of Medicine, Department of Medicine, Cardiology, La Jolla, CA 92093, USA.

*Author for correspondence (rross@ucsd.edu)

Received 1 October 2013; Accepted 4 December 2013

Journal of Cell Science

Journal of Cell Science (2014) 127, 1104–1116 doi:10.1242/jcs.143743

Gap junctions allow for rapid conductance of action potentials and therefore electrically couple cardiac myocytes (Delmar and Liang, 2012; Rhett et al., 2011; Saffitz et al., 2000). They further permit intercellular transport of ions and small biologically active molecules, thereby coordinating physiological processes such as cell differentiation, growth regulation and cell death (Decrock et al., 2009; Kardami et al., 2007). It has been proposed that ZO-1 controls the rate of Cx43 accretion at gap junction peripheries, thereby regulating gap junction size and distribution (Hunter et al., 2005). Previous reports have suggested that Cx43 found in the area surrounding a gap junctional plaque, also referred as the perinexus, colocalizes with ZO-1 and regulates the abundance of Cx43 available for incorporation into the gap junctional plaques (Rhett and Gourdie, 2012; Rhett et al., 2011).

Vcl has been linked to important functions within the cardiac myocyte. It is highly expressed at costameres and intercalated discs and has been shown to be important for the determination of cell shape as well as ordered assembly and alignment of cardiac myofibrils (Shiraishi et al., 1997). Global deletion of the mouse *Vcl* gene causes embryonic growth retardation with lethality by E10. Vcl-null embryos have multiple defects including abnormal cardiogenesis (Xu et al., 1998). We previously studied hemizygous null Vcl mice and showed that normal Vcl expression is essential for cardiac adaptation to pressure-overload (Zemljic-Harpf et al., 2004). In addition we investigated the role of Vcl in the heart by means of cardiac-myocyte-specific inactivation of the mouse *Vcl* gene (cVclKO). These cVclKO mice developed two distinct phenotypes; a subset of them displayed ventricular tachycardia and died suddenly within the first 10 weeks of life, despite preserved systolic cardiac function. cVclKO mice that survived past this period, developed dilated cardiomyopathy and died of heart failure by 6 months of age (Zemljic-Harpf et al., 2007). Importantly, abnormal distribution of gap junctional protein Cx43 was detected within the intercalated discs of both $Vcl^{+/-}$ and cVclKO mice when the mouse heart function was normal (Zemljic-Harpf et al., 2007; Zemljic-Harpf et al., 2004). Given these findings in the mouse heart, we hypothesized that Vcl and ZO-1 interact, and that loss of this interaction would destabilize Cx43-containing gap junctions, perturb gap junction function and cause abnormalities in myocyte integrity.

RESULTS

Vcl is necessary for ZO-1 localization to the intercalated disc

In previous studies, we have demonstrated that decreased levels of Vcl in cardiac tissue are linked to alterations in Cx43 levels (Zemljic-Harpf et al., 2007; Zemljic-Harpf et al., 2004). Hence, we first assessed ZO-1 in normal cardiac tissue. Given its known expression in capillary endothelium, we performed immunofluorescence staining with antibodies for both ZO-1 and the endothelial-cell-specific marker PECAM. ZO-1 had a longitudinal expression pattern in capillary endothelial cells, adjacent to cardiac myocytes (Fig. 1A). In addition ZO-1 was seen in a transverse pattern corresponding to localization at the cardiac myocyte intercalated disc (Fig. 1A, asterisks). Given that ZO-1 is a known Cx43 interacting partner, we next assessed whether Vcl and ZO-1 colocalized in cardiac tissue. Immunostaining of transverse sections suggested that there was Vcl and ZO-1 colocalization in normal cardiac tissue (Fig. 1B, asterisks).

Next, we assessed whether proper Vcl expression was necessary for ZO-1 positioning in the intercalated disc. Heart tissue from the cardiac-myocyte-specific Vcl-knockout (cVclKO) mice was used and we found that when Vcl was absent from cardiac myocytes, ZO-1 was no longer detected at the intercalated disc (Fig. 1C). Given that cVclKO mice lacked Vcl only in cardiac muscle cells, Vcl and ZO-1 were still detected in endothelial cells within the capillary bed, and were also visualized in non-myocytes within the heart (Fig. 1C, double asterisks).

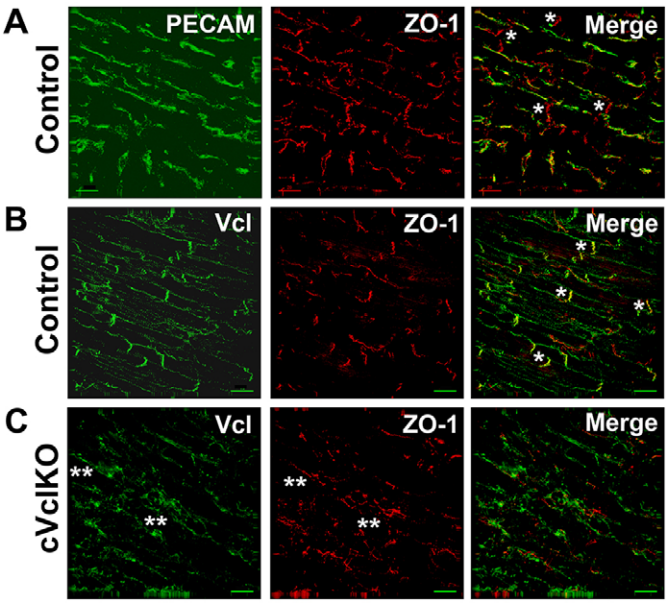

Fig. 1. Vcl and ZO-1 colocalize at intercalated discs in wild-type cardiac myocytes and when Vcl is deleted from cardiac myocytes ZO-1 is also lost. (A,B) Wild-type mouse heart tissue was evaluated by immunomicroscopy using anti-PECAM and anti-ZO1 antibodies (A), or anti-Vcl and anti-ZO-1 antibodies (B). PECAM staining showed a longitudinal staining pattern consistent with marking endothelial cells between cardiac myocytes. This PECAM expression highlights the substantial endothelial cell ZO-1 expression adjacent to cardiac myocytes. Within the cardiac myocytes, ZO-1 is distinctly at the intercalated disc, and ZO-1 and Vcl colocalize (*). Scale bar: 20 μm. (C) cVclKO heart tissue was evaluated with immunomicroscopy using anti-Vcl and anti-ZO-1 antibodies. ZO-1 and Vcl where detected in endothelial cells and non-myocyte cell populations (**). Upon cardiac-myocyte-specific *Vcl* gene deletion (cVclKO), Vcl expression was lost from the cell and ZO-1 expression was lost in parallel. Note there are no easily visualized intercalated discs when compared to controls.

To further show that Vcl and ZO-1 colocalized at the intercalated disc, we used isolated adult cardiomyocytes. Colocalization was again seen at intercalated discs (Fig. 2A, asterisks). Patchy ZO-1 expression was detected on the lateral sarcolemma owing to the 'step-like' arrangement of the intercalated discs (Fig. 2A, asterisks), but no colocalization could be identified at lateral Vcl-containing cell adhesion sites (Fig. 2A, double asterisk). Taken together, these findings indicate that ZO-1 is primarily expressed at cardiomyocyte-to-cardiomyocyte intercalated disc connections, where it colocalizes with Vcl, and that normal Vcl expression is necessary for proper expression and positioning of ZO-1 at the intercalated disc.

Vcl directly interacts with ZO-1

ZO-1 is known to directly bind to Cx43 in cardiac myocytes (Giepmans and Moolenaar, 1998; Toyofuku et al., 1998). Given our findings above and our prior data showing that Vcl expression

Journal of Cell Science (2014) 127, 1104–1116 doi:10.1242/jcs.143743

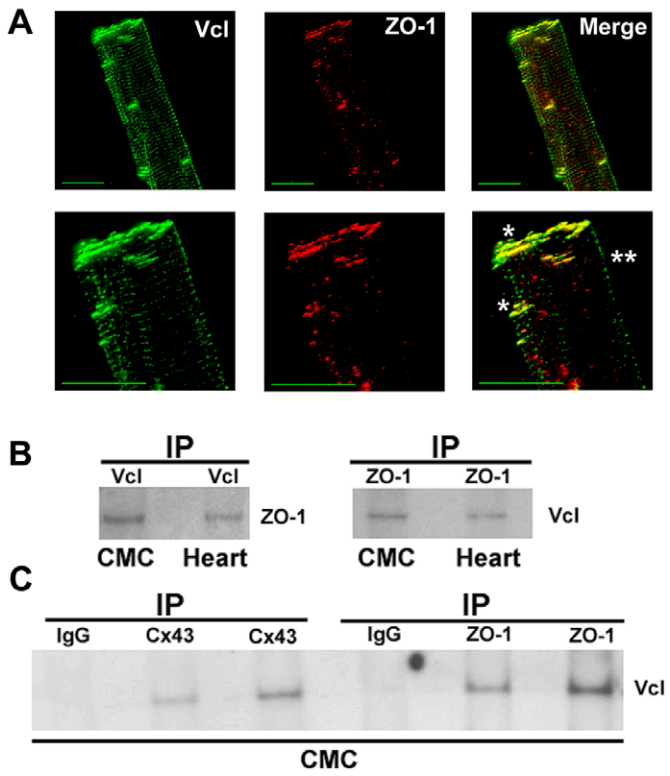

Fig. 2. Vcl, Cx43 and ZO-1 form a scaffolding complex in cardiac myocytes. (A) Vcl and ZO-1 colocalize in intercalated discs of isolated cardiac myocytes. Upper panel: Vcl and ZO-1 colocalize at the intercalated disc of wild-type cardiac myocytes. The apparent lateral expression of ZO-1 was owing to the known staggered 'step-like' arrangement of the intercalated disc. No colocalization was found along the non-intercalated disc sarcolemmal membrane. Lower panel: the enlarged image of the intercalated disc and the lateral cell wall of cardiac myocytes showed colocalization of Vcl and ZO-1 in yellow at the intercalated disc (*) but not at the lateral cell border (**). Scale bars: 20 μm. (B) Vcl and ZO-1 co-immunoprecipitate in whole heart and isolated cardiac myocytes. Protein lysates from wild-type mouse whole heart (Heart) or isolated cardiac myocytes (CMC) were co-immunoprecipitated (IP) with anti-Vcl, anti-ZO-1 or anti-Cx43 antibodies. Then the Vcl-IP and ZO-1 IP samples were subjected to immunoblot analyses with either anti-ZO-1 or anti-Vcl antibodies, respectively. (C) Wild-type whole heart lysates were further used to show that Vcl formed a complex with Cx43 and ZO-1. Cx43 IP and ZO-1 IP samples were subjected to Vcl immunoblotting using an anti-Vcl antibody. IgG was used as a negative control.

is necessary for proper Cx43 placement in the cardiac muscle (Zemljic-Harpf et al., 2007), we investigated whether ZO-1 and Vcl proteins bind directly to each other. First, we performed reciprocal immunoprecipitation studies using anti-Vcl, anti-ZO-1 and anti-Cx43-specific antibodies with cardiac tissue and cardiomyocyte lysates. Our results showed that Vcl, Cx43 and ZO-1 form a complex in both the whole heart and isolated cardiac myocytes (Fig. 2B,C).

Next, we performed a yeast two-hybrid (Y2H) interaction screen to test for direct interaction of Vcl and ZO-1. We designed a series of Vcl bait constructs spanning the full-length of Vcl, and also constructed ZO-1 prey sequences spanning the 5′ 2.5 kb of the full-length ZO-1 transcript (Fig. 3A). β-galactosidase assays revealed that full-length Vcl and the N-terminal Vcl domain both interacted with the first 2.5kb of ZO-1 (Fig. 3B). Of note, we did not find any interaction between Vcl fragments and the C-terminal domain of ZO-1 (the region coded for by the 2.5–5.2 kb portion of ZO-1) (data not shown). To identify a minimal interacting domain in ZO-1, we performed additional Y2H analysis using a series of smaller fragments of the ZO-1 coding sequence as bait, against full-length Vcl as prey (Fig. 3C). β-galactosidase activity assays revealed that only fragments containing the third PDZ domain, or the third PDZ plus SH3 domains of ZO-1, interacted with Vcl (Fig. 3D). Taken together, these findings indicate that Vcl directly binds to ZO-1 in adult cardiac myocytes, and thereby forms a scaffolding complex with ZO-1 and Cx43.

Vcl ablation reduces protein expression of Vcl-associated proteins as well as that of Cx43

To further elucidate how Vcl might control Cx43 expression in cardiomyocytes we turned to a cell culture system using neonatal mouse ventricular myocytes (NMVMs) isolated from Vcl homozygous 'floxed' ($Vcl^{fl/fl}$) mouse hearts, in which the *Vcl* gene could be deleted. To ensure pure NMVMs were evident in our cultures, cells were immunolabeled with the cardiac-myocyte-specific anti-sarcomeric-α-actinin antibody, and colabeled with an anti-Cx43 antibody. For our experimental design, it was crucial that Cx43 and Vcl were both expressed at the sarcolemma because we wanted to test whether Vcl reduction would affect the membrane localization of Cx43. We expected a prominent membrane-localized Cx43 staining pattern in NMVMs but found that when NMVMs were grown in sparse culture conditions, they only displayed intense perinuclear Cx43 expression and sparse membrane localization (Fig. 4A). In contrast, when cells were grown at higher densities, they formed contact sites, and Cx43 was seen at cell-to-cell contacts (Fig. 4B). Confluent NMVMs formed an intact monolayer in which Cx43-containing cell–cell contacts were detected along the cell membrane, more akin to *in vivo* conditions in cardiac tissue (Fig. 4C). Based on these findings, we utilized confluent culture conditions for the remainder of this study.

To reduce Vcl expression in this model system, we infected NMVMs derived from $Vcl^{flox/flox}$ mice with a recombinant adenovirus (AdV) expressing Cre-recombinase (AdV-Cre). Cells infected with a recombinant AdV expressing β-galactosidase (AdV-LacZ) served as controls (Iwatate et al., 2003). To further control for any potential side effects owing to AdV-Cre treatment alone, we also used wild-type (WT) NMVMs (no floxed Vcl allele) and exposed them to AdV-Cre. No change in Vcl protein expression or morphology was detected in these AdV-Cre-infected WT NMVMs (supplementary material Fig. S1). Immunoblotting and RT-PCR studies were performed on samples from AdV-Cre- or AdV-LacZ-infected $Vcl^{flox/flox}$ NMVMs. In initial studies, we found that Cre-infected $Vcl^{flox/flox}$ cells maintained for 72 h or longer detached from matrix-coated plates, as the Vcl protein levels became profoundly reduced (data not shown). Therefore, to analyze Vcl-deficient and control cells that were morphologically similar and remained well attached to matrix, we used cells at ~60 h post-infection. At this 60-h time point Cre-mediated Vcl gene excision caused Vcl protein and transcript expression to be reduced to 51±4% ($P<0.01$) and 27±2% ($P<0.0001$), of control infected cell values, respectively (Fig. 5A,B). With Vcl protein reduction, we found significantly reduced expression of Vcl-associated proteins, including: ZO-1 (61±2%, $P<0.0001$), Cx43 (17±8%, $P<0.0001$), β1D integrin (21±1%, $P<0.0001$), talin (43±6%, $P<0.0001$), and tubulin (21±3%, $P<0.001$), values being expressed relative to control values and normalized to GAPDH (Fig. 5A). The levels of

Journal of Cell Science (2014) 127, 1104–1116 doi:10.1242/jcs.143743

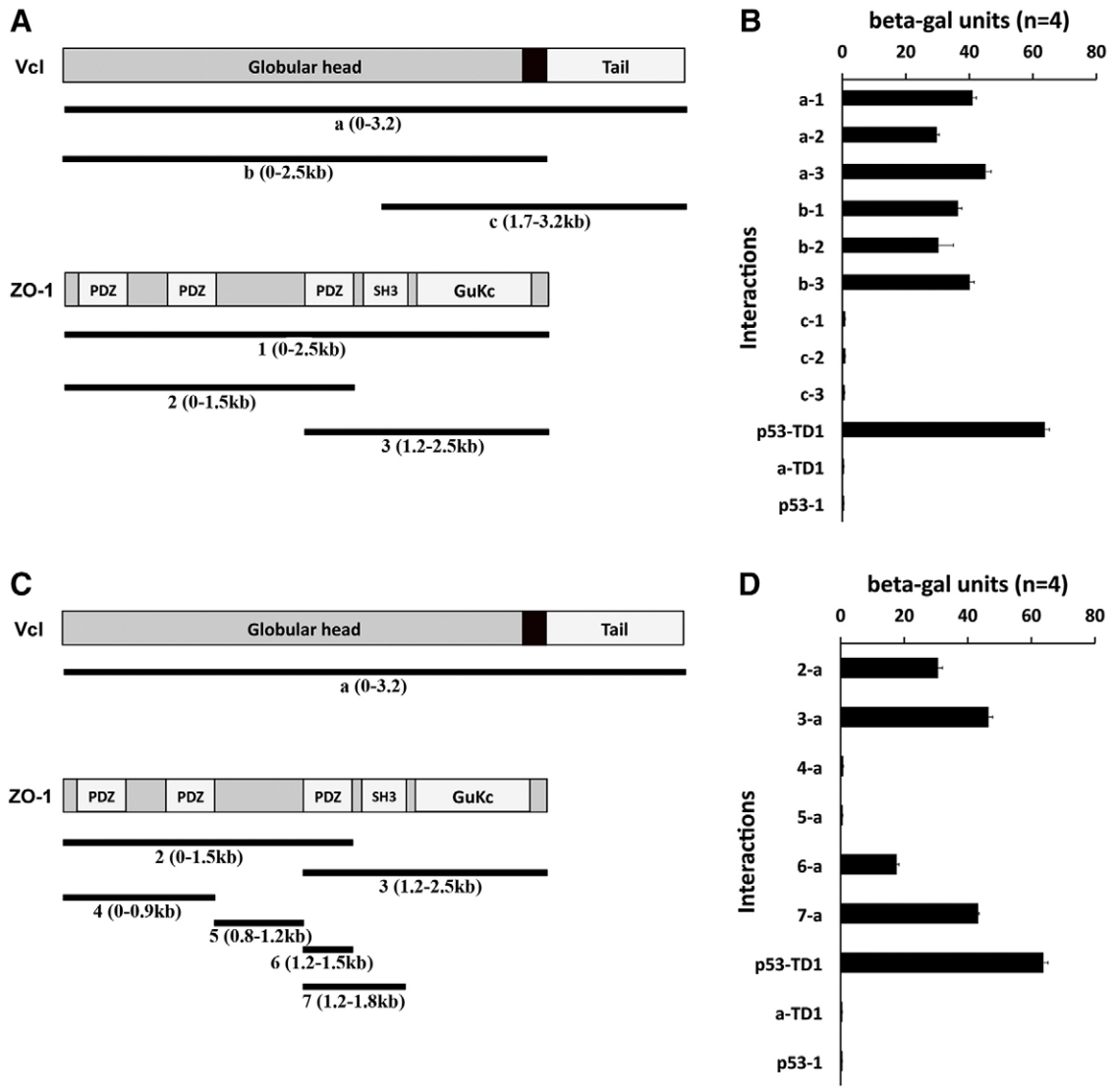

Fig. 3. Yeast two-hybrid screening showing that Vcl directly interacts with ZO-1. (A) Schematic representation of Vcl (head, gray; hinge, black; and tail, white) and ZO-1 fragments used to assay for protein interaction. Constructs were made based on coding sequences for full-length Vcl (0–3.2 kb), and deletion mutants of Vcl (0–2.5 kb and 1.6–3.2 kb), and used as bait in yeast two-hybrid assays. These are labeled as a, b and c. Constructs based on coding sequences for ZO-1 (0–0.25 kb, 0–1.5 kb and 1.5–2.5 kb) were used as prey and labeled as 1, 2 and 3. (B) β-galactosidase activity assays revealed that the N-terminal region of Vcl interacted directly with ZO-1. Graphical results show that full-length Vcl interacted with ZO-1 (assays a-3 and a-2). The N-terminal Vcl domain also interacted with ZO-1 (assays b-3 and b-2). In contrast the C-terminal Vcl domain did not interact with ZO-1 (assays c-3 and c-2). (C) Schematic representation of additional constructs used to refine the Vcl–ZO-1 interactions in a second set of yeast two-hybrid experiments. Here, a full-length Vcl (0–3.2 kb) construct was used as prey and designated as construct 'a'. Constructs produced from partial coding sequences for ZO-1 were used as bait and designated as fragments 2–7. (D) Only fragments of ZO-1 containing the third PDZ (2 and 6) or the third PDZ plus SH3 domains (3 and 7) interacted with Vcl. Positive controls were p53-TD1 and negative controls were a-TD1 and p53-1.

transcripts of these Vcl-associated proteins were not significantly changed compared to controls (Fig. 5B). These data indicate that Vcl controls not only Cx43 protein expression and function in cardiac myocytes, but that, as Vcl is lost from the cell, protein expression of a range of Vcl-related proteins is also perturbed.

Vcl reduction causes a decrease in gap junctional communication

Immunohistochemical analysis was next performed in this cell culture model. As above, cells were analyzed at ~60 h post-infection. Upon the reduction of Vcl protein, membrane localization of Cx43 was lost (Fig. 6A). To specifically assess gap junction function and intracellular communication between connecting NMVMs, we then performed dye microinjection studies as well as scrape loading assays (Boswell et al., 2009; el-Fouly et al., 1987; Li et al., 2011; Opsahl and Rivedal, 2000) (Fig. 6B,C) . For these studies we used two dyes: Lucifer Yellow, which can be transported easily through gap junctions, and Rhodamine dextran, which is too large to pass directly through gap junctions (Fig. 6B). When we performed simultaneous microinjection of Rhodamine dextran and Lucifer Yellow into NMVMs, control cells ($Vcl^{fl/fl}$ plus AdV-LacZ) showed extensive Lucifer Yellow dye transfer to adjacent NMVMs, but no transfer

Journal of Cell Science (2014) 127, 1104–1116 doi:10.1242/jcs.143743

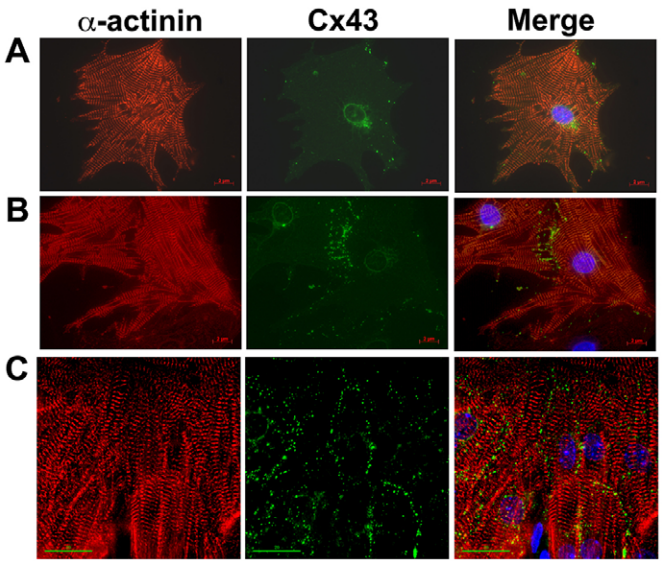

Fig. 4. Membrane localization of cardiac myocyte Cx43 requires dense culture conditions to allow formation of cell–cell junction sites. Cardiac myocytes were colabeled with anti-sarcomeric α-actinin and anti-Cx43 antibodies. (A) Sparsely plated cells showed dominant perinuclear Cx43 expression and only weak expression of Cx43 along the sarcolemma. (B) When cardiomyocytes were in close cell–cell contact, sarcolemmal-localized Cx43 expression was found only at cell–cell contact sites. (C) Confluent cultures display strong Cx43 expression along the whole sarcolemma, marking cell-to-cell adhesion sited. Scale bars 2 μm (A,B), 20 μm (C,D).

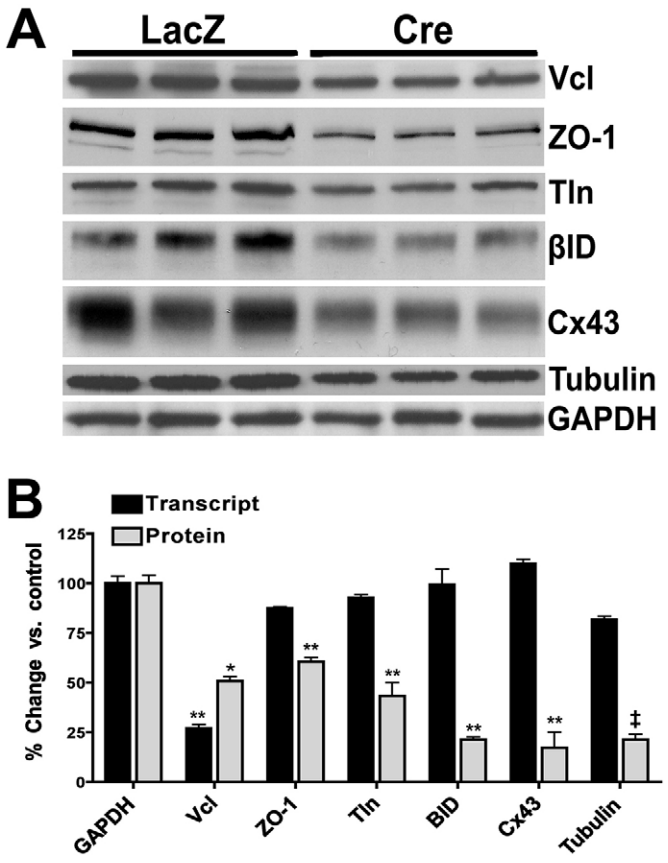

Fig. 5. Reduction of Vcl protein in cardiac myocytes alters expression of a range of associated proteins. (A) Immunoblotting revealed that AdV-Cre infection of Vcl$^{fl/fl}$ (VclKO) neonatal mouse ventricular myocytes reduced Vcl protein expression to 51%±4, *P<0.01, compared to control (AdV-LacZ) infected Vcl$^{fl/fl}$ cardiomyocytes. With this we found protein expression of the Adv-Cre infected cells compared to control infected cells was reduced as: ZO-1 (61±2%, **P<0.0001), Cx43 (17±8%, **P<0.0001), talin (43±6%, **P<0.0001), β1D integrin (21±1%, **P<0.0001) and tubulin (21%±3%, ‡P<0.001). GAPDH protein expression was unchanged and used as loading control. (Densitometric analyses of the individual proteins were all normalized to GAPDH and these data are displayed in Panel B together with transcript analysis.) (B) qRT-PCR was used to assay samples from Vcl$^{fl/fl}$ cardiomyocytes in which Vcl was reduced as above via AdV-Cre infection. At 56 h post infection, Vcl transcript expression, normalized to GAPDH transcript, was reduced by Cre-mediated gene excision (27±2% of control, **P<0.0001). However, Vcl reduction in cardiac myocytes did not significantly alter the transcript levels of the associated cardiac myocytes proteins, ZO-1, talin, β1D integrin, Cx43 or tubulin when compared to AdV-LacZ-treated control cells. Densitometric analysis of protein expression from panel A is shown here to allow direct comparison with transcript expression in the same samples.

of Rhodamine dextran, whereas the Vcl-deficient cells (Vcl$^{fl/fl}$ plus AdV-Cre) showed little Lucifer Yellow dye transfer to neighboring cells (Fig. 6B).

To further evaluate gap junction communication, we also performed a companion assay in our culture system with scrape loading of the Lucifer Yellow and Rhodamine dextran dyes (Fig. 6C). Control cells (Vcl$^{fl/fl}$ plus AdV-LacZ) showed Lucifer Yellow transfer to cells distant from the scratch, indicating appropriate gap junction function, whereas Vcl-deficient cells (Vcl$^{fl/fl}$ plus AdV-Cre) displayed Lucifer Yellow dye transfer only to cells adjacent to the scratch, indicating that no significant gap junctional communication took place. Taken together, microinjection and scrape-loading data indicate that proper Vcl expression in cardiac myocytes is necessary for appropriate gap junction function.

Vinculin disruption inhibits PI3K/PTEN signaling in cardiac myocytes

Given that we found that Vcl, ZO-1 and Cx43 interacted, and that loss of Vcl reduced expression of ZO-1, Cx43 and β1D integrin protein, we next evaluated how loss of myocyte Vcl affected key signaling molecules necessary for cardiomyocyte homeostasis.

For this, we chose first to assess PI3K, phosphatase and tensin homolog (PTEN) expression and proteins in downstream survival signaling pathways (e.g. Akt and ERK1/2). Whole-cell lysates derived from AdV-Cre- and AdV-LacZ-infected Vcl$^{fl/fl}$ NMVMs were analyzed (Fig. 7A). When Vcl was reduced in these cells, reduced levels of PI3K phosphorylated on Y458 PI3K$^{(Y458)}$ (0.70±0.03, P<0.05), PTEN (0.60±0.11, P<0.05) and total Akt (0.42±0.09, P<0.005), all fold-change relative to GAPDH, compared between LacZ and Cre samples, were detected. Interestingly, phosphorylated pAkt^{S473} and pAkt^{T308} were independently increased, as total Akt was significantly reduced, in the Vcl-deficient cells. This yielded an increase in normalized Akt^{T308}/tAkt (4.00±0.32, P<0.001) and Akt^{S473}/tAkt (5.94±0.08, P<0.0001) versus control samples. Vcl reduction also induced fold changes in ERK1 (2.10±0.07, P<0.001) and ERK2 activation (4.65±0.06, P<0.001), when normalized to total ERK1/2 expression (Fig. 7A,B). The membrane- and actin-cytoskeleton-associated proteins α-actinin, β-catenin and dystrophin were not affected by Vcl deficiency, but RhoA kinase protein expression was significantly reduced (Fig. 7C,D). These data indicate that reduction of Vcl in the NMVM leads to

Journal of Cell Science (2014) 127, 1104–1116 doi:10.1242/jcs.143743

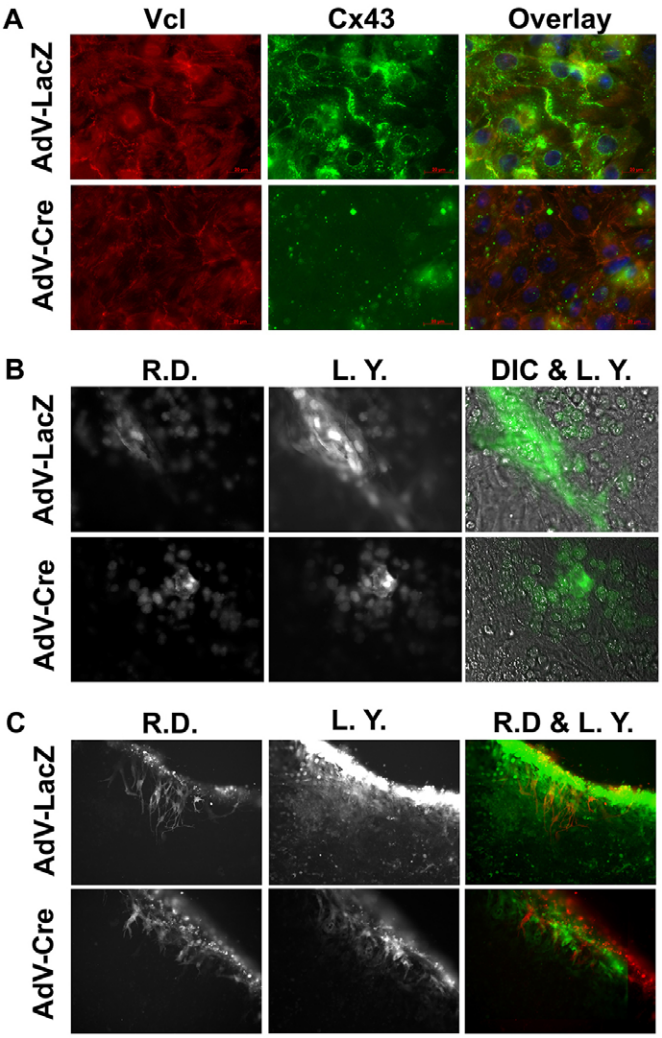

Fig. 6. Vcl reduction in NMVMs disrupts Cx43 protein localization, and ZO-1 and Cx43 expression, and causes dysfunctional cell–cell communication. (A) Immunomicroscopy shows that reduction of Vcl expression in $Vcl^{fl/fl}$ NMVMs using adenoviral Cre (AdV-Cre) results in significant visible reduction of Cx43 protein expression compared to AdV-LacZ-infected control cells. Loss of Cx43 from both perinuclear and cell–cell contact sites was found in VclKO. (B) After simultaneous microinjection of Rhodamine dextran (R.D.) and Lucifer Yellow (L.Y.) into NMVMs, evaluation of dye transfer to neighboring cells was observed. Rhodamine dextran labeled the injected cardiac myocytes. Control cells (AdV-LacZ) showed extensive Lucifer Yellow dye transfer to adjacent cardiac myocytes consistent with functional gap junctions, but Vcl-deficient cells (AdV-Cre) showed no Lucifer Yellow dye spreading to neighboring cardiomyocytes, indicating reduced gap junction function in the Vcl-deficient cells. (C) Scrape loading assays using Rhodamine dextran and Lucifer Yellow dyes. Rhodamine dextran marked the cell scrape loading, consistent with cell injury. Lucifer Yellow dye transfer only took place in AdV-LacZ control cells, but not in AdV-Cre-treated Vcl-deficient cultures, again showing defective gap junction communication in the Vcl-deficient cardiac myocytes.

altered signaling through PI3K/PTEN, with associated activation of both Akt and ERK1/2.

Vcl reduction causes rapid cellular injury

PI3K activation plays an important role in myocardial metabolism, pro-survival signaling and cardiac contractility, and normal gap junction function is essential for cellular growth, proliferation and survival (Decrock et al., 2009; Kardami et al., 2007). Given that our above studies show that Vcl loss from myocytes results in disturbed expression of Cx43, gap junction function and survival signaling, we next evaluated how loss of myocyte Vcl affects cell death pathways.

Our previous studies in whole heart revealed excessive replacement fibrosis in cVclKO mouse hearts, consistent with death and loss of cardiac myocytes (Zemljic-Harpf et al., 2007). Furthermore, as discussed above, upon a reduction of Vcl protein of >50% of normal amounts (greater than 60 h in our culture system) we found that NMVM had cell shrinkage and detached from matrix-coated plates (data not shown). Given this combined information, we next evaluated whether Vcl reduction in the NMVM system triggered activation of either apoptotic or autophagic cell death pathways. With reduced Vcl expression, expression of the apoptotic markers PARP and cleaved caspase 3 were inhibited (Fig. 7E,F). In parallel with reduction of Vcl protein, we detected reduced Beclin-1 and LC3 protein expression (Fig. 7E,F).

Lactate dehydrogenase (LDH) is only released from cells when the plasma membrane is damaged. Therefore to assess for a potential cytotoxic effect of Vcl protein reduction, we measured LDH release by the cells into culture medium. Increased LDH release was detected in the Vcl-deficient cells as compared to controls (Fig. 7G). Cell morphology was visually checked every 12 h, and smaller cell size as well as areas of cellular lysis were visible by 72 h post AdV infection; no similar changes in morphology were evident in AdV-LacZ-treated control cells (Fig. 7H). Our data indicate that reduced Vcl expression does not induce apoptotic or autophagic signaling events, but induces necrotic cell death by plasma membrane injury, as documented by increased LDH release.

DISCUSSION

We report here for the first time that: (1) Vcl colocalizes with ZO-1 at the intercalated disc of cardiac myocytes, (2) there is a direct interaction between the Vcl head domain and the third PDZ domain of ZO-1, (3) reduced Vcl expression in the cardiomyocyte results in a loss of Cx43 and ZO-1 expression, as well as their localization, and (4) reduced VCL expression perturbs gap junctional intercellular communication, as well as downstream PI3K-dependent signaling. This leads to an increased cardiac myocyte mortality by necrotic processes. Our data suggest that Vcl, Cx43 and ZO-1 form a protein complex at the intercalated disc that ensures normal gap junction function and myocyte survival.

Novel role of Vcl in gap junctional communication

The localization of Vcl at costameres and its involvement in focal adhesion formation and maturation is well known (Craig and Pardo, 1983; Dumbauld et al., 2013; Pardo et al., 1983). Vcl can regulate the coupling of adhesion sites to the actin cytoskeleton (Chandrasekar et al., 2005), and is also known for binding to cadherin-based cell–cell contact sites through α- and β-catenin (Peng et al., 2010; Weiss et al., 1998). Recently it has been described that ZO-1 recruitment to α-catenin links the assembly of the endothelial barrier to adherens junctions (Maiers et al., 2013). Desmosomes are localized at the intercalated disc and link intermediate filaments to the muscle termini via desmoplakin, plakophilin and plakoglobin. Both fascia adherens and desmosomes form mechanical linkages, bridging the contractile apparatus of adjacent myocytes, thereby strengthening the

Journal of Cell Science (2014) 127, 1104–1116 doi:10.1242/jcs.143743

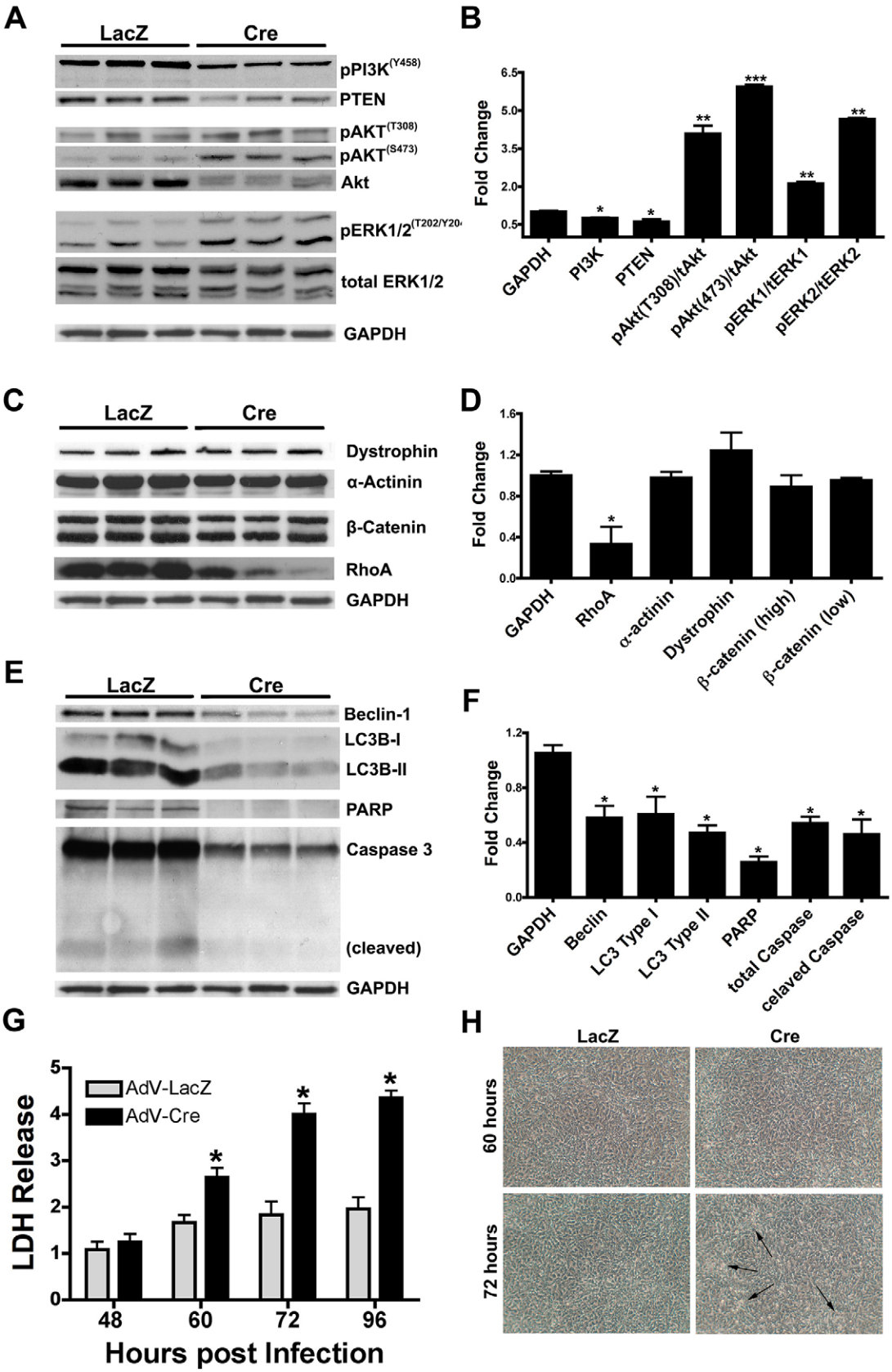

Fig. 7. See next page for legend.

Journal of Cell Science (2014) 127, 1104–1116 doi:10.1242/jcs.143743

Fig. 7. Vcl disruption causes reduced PI3K activation, but increased activation of Akt and ERK 1/2 in cardiac myocytes. (A,B) Western blot (A) and densitometric analysis (B) of control (LacZ) and AdV-Cre (Cre) infected NMVMs. With AdV-Cre expression in $Vcl^{fl/fl}$ NMVMs, reduction in fold changes, relative to GAPDH, were noted in phosphorylated $PI3K^{(Y458)}$ (0.70±0.03, *P<0.05) and PTEN (0.60±0.11, *P<0.05) proteins. In addition, increases (fold-changes relative to GAPDH) were observed in $pAkt^{T308}$/tAkt (4.00±0.32 32%, **P<0.001) and Akt^{S473}/tAkt (5.94±0.08, ***P<0.0001), pERK1/tERK1 (2.10±0.07,**P<0.001) and pERK2/tERK2 (4.65±0.06, **P<0.001). (C,D) The Vcl associated proteins α-actinin, β-catenin and dystrophin were not affected by Vcl deficiency, but RhoA kinase protein expression was significantly reduced 0.33±0.17 fold, relative to control (*P<0.05). (E,F) Compared to control cells, the fold change of the autophagy markers Beclin-1 and LC3 were reduced in Vcl-deficient cells (Beclin 0.58±0.09, LC3 Type I, 0.61±0.13, and LC3 Type II, 0.47±0.06). Decreased Vcl protein in NMVM, further inhibited the fold expression of total caspase 3 (0.54±0.05), as well as the apoptotic markers PARP (0.25±0.04) and cleaved caspase 3 (0.46±0.11), relative to control. All values *P<0.001, relative to GAPDH, vs. control. (G) AdV-Cre-induced Vcl reduction leads to increased LDH release into the cardiomyocyte culture medium, when compared to AdV-LacZ-treated controls (*P<0.001). (H) Bright field images of floxed Vcl NMVM showing that at 60 h post infection NMVM are undistinguishable from controls, but 72hs AdV-Cre infection leads to alterations in cellular morphology.

connection between adjoining cells. Current literature states that Vcl is present in integrin-containing cell-to-matrix junctions as well as cadherin-based cell-to-cell adhesion sites (Fig. 8A). Gap junctions are also found at intercalated discs (Fig. 8A). Cx43-containing gap junctions are known to regulate intercalated disc function (Delmar and Liang, 2012). Whereas Cx43 directly binds to ZO-1 in cardiac myocytes (Giepmans and Moolenaar, 1998; Toyofuku et al., 1998), this interaction is not apparent in seminiferous epithelium, suggesting that the Cx43 interaction with ZO-1 occurs in a cell-type-specific manner (Li et al., 2009).

Global deletion of ZO-1 in mice results in abnormal angiogenesis, pericardial effusions (suggesting *in utero* heart failure) and mid-gestation lethality by E11.5 (Katsuno et al., 2008). Therefore, this model could not be used to address the role of ZO-1 in postnatal cardiac myocytes. Future studies that use cardiac-myocyte-specific-knockout studies of ZO-1 would be useful to compare with our Vcl cardiomyocyte knockout data. It is important to mention that global Vcl-knockout embryos die by E10, also presenting with a thin-walled myocardium and pericardial effusions.

Our novel data presented here indicate that a Vcl–ZO-1–Cx43 complex forms in cardiac myocytes and that Vcl directly interacts with ZO-1. This study is the first to report that Vcl directly interacts with ZO-1, and in doing so, regulates gap junctional positioning and function (Fig. 8A, red circle). Given that it is known that ZO-1 directly interacts with α-catenin (Müller et al., 2005), and our study shows that Vcl binds ZO-1, we propose that Vcl might function as a molecular linker between adherens and gap junctions. The data in our myocyte culture model showed that even a mild reduction of Vcl protein caused decreased ZO-1, Cx43 and β1-integin protein expression, suggesting that Vcl is a crucial actin cytoskeletal linker that plays an important role in membrane localization of β1-integrin and Cx43 (Fig. 8A, red circle). Taken together, data here suggests that if a mutant Vcl or reduced amount of wild-type Vcl were present in the cardiac myocyte, Cx43 positioning in the gap junction, and ultimately, gap junction function, would be perturbed (Fig. 8B).

Novel role of Vcl in PI3K/Akt signaling

Vcl interacts with phospholipids in the plasma membrane, by directly binding PIP_2. It is known that PI3K regulates the coupling of adhesion sites to the actin cytoskeleton. Because of this, it plays a role in apoptotic cell death by activating pro-survival signaling pathways and reducing PIP_3 signaling. In fibroblasts, Vcl has been shown to regulate integrin adhesion turnover, and reduced Vcl expression resulted in smaller and less abundant focal adhesions (Saunders et al., 2006). This study suggested that Vcl inhibits cell migration by stabilizing focal adhesions, and that binding of inositol phospholipids to the Vcl tail plays an important role in focal adhesion turnover.

A key molecule downstream of PI3K is the serine/threonine kinase Akt. Apoptosis is associated with physiological or programmed cell death, in contrast to necrosis, which is associated with cell injury. As we investigated the role of Vcl in the ZO-1–Cx43 axis using the NMVM model, we noted that even a modest reduction of Vcl led to rapid cell death. Therefore we investigated how Vcl might alter signaling pathways that have been linked to cell survival of cardiomyocytes, such as the PI3K pathway. We were especially interested in the PI3K pathway because Vcl has been shown previously to control PTEN levels in embryonic fibroblasts (Subauste et al., 2005). PTEN is known to regulate PI3K/Akt and even ERK1/2, although much of this work has been performed in cancer cells (Chetram and Hinton, 2012). In addition, PI3K has been shown to protect against heart failure following myocardial infarction in mice (Lin et al., 2010). It has further been suggested that exercise enhanced PI3K (p110α) activity could delay or prevent progression of dilated and hypertrophic cardiomyopathy (McMullen et al., 2007). Finally, a recent study has described that PI3K(p110α) gene therapy reduced cardiac dysfunction (Weeks et al., 2012). Our studies here show that reduction of Vcl levels in cardiac myocytes reduced PI3K activation, and inhibited autophagic and apoptotic signaling, compared to control cells with normal Vcl expression. A component of this cell death might have been induced by inhibition of PI3K activation due to reduced Vcl protein expression. In addition, because Vcl links the sarcolemma to the actin cytoskeleton, Vcl deficiency could have also led to structural instability of the cardiac myocyte membrane. Together, because Vcl modifies both of these crucial properties in the myocyte, its loss leads to cellular dysfunction and necrosis.

Traditionally, PI3K activation leads to phosphorylation of Akt, thereby regulating the activity of several cellular processes including transcription, cell proliferation, glucose metabolism, apoptosis and cell migration (Katso et al., 2001; Song et al., 2005). Our studies here have shown that reduced Vcl inhibited PI3K activation in cardiac myocytes. Unexpectedly we also found hyperphosphorylation of Akt^{S473} and Akt^{T308} together with reduced total Akt levels. It is known that phosphorylated Akt undergoes rapid degradation, but why Akt activation occurred in our model, while PI3K activation was reduced, remains unclear. Usually Akt activation is considered to induce pro-survival and anti-autophagy signals. Our data suggest that Vcl deficiency induced cellular stress responses to trigger Akt activation as a compensatory mechanism for compromised cytoskeletal function. Increased Akt phosphorylation has also been shown in other studies where skeletal muscle cells were serum starved (Ching et al., 2010). Rho kinase inhibition in mouse brain, maintained Akt but decreased PTEN activity, and inhibited caspase-3 activity (Wu et al., 2012). A recent study describes that interference with Akt1 signaling in all cells *in vivo*, reduced cardiac dysfunction, hypertrophy and cardiac fibrosis, thereby improving survival in a mouse model of spontaneous myocardial infarction (Kerr et al., 2013). Most relevant for our study here is that Cx43 was shown to

Journal of Cell Science (2014) 127, 1104–1116 doi:10.1242/jcs.143743

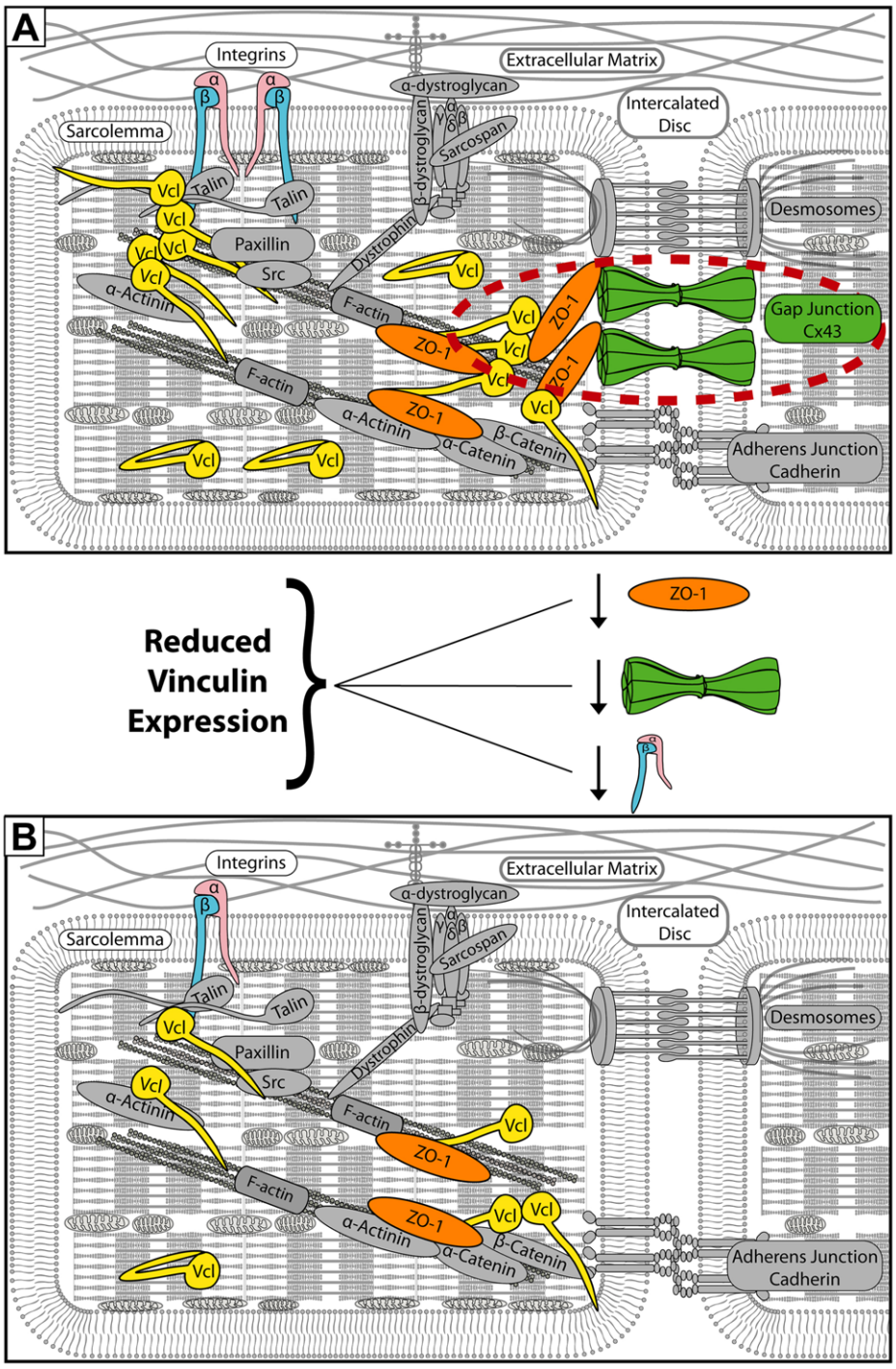

Fig. 8. Diagrammatic representation of Vcl and its associated proteins. Vcl is located at cell-to-cell intercalated discs as well as cell-to-matrix adhesion sites, thereby linking the actin cytoskeleton to the plasma membrane. Our novel findings suggest that Vcl also binds through ZO-1 to Cx43-containing gap junctions. Thereby, Vcl acts as a mechanical linker between gap junctions and adherens junctions localized at the intercalated disc in the plasma membrane, but at the same time Vcl cross-links the actin cytoskeleton, thereby anchoring actin filaments to the sarcolemma. (A) The red circle highlights the novel interaction between Vcl, ZO-1 and Cx-43 identified in this study. (B) Vcl reduction results in a loss of membrane-localized gap junctions, as well as reduced protein expression of ZO-1 and β1D integrin. At the intercalated disc, reduced Vcl protein affects gap junction localization and function. At cell-to-matrix connection sites, decreased Vcl protein expression weakens integrin-based cell adhesion.

contribute to the activation of the PI3K/Akt signaling pathway in cardiac myocytes (Ishikawa et al., 2012).

Vcl regulation as a novel target to prevent or induce cell death

Our study found that a reduction of Vcl protein of >50% of normal amounts led to NMVM detachment from matrix-coated plates. In cardiac muscle, the costamere forms the intersection between the extracellular matrix and the cellular cytoskeleton, and is a pivotal point for transmission of mechanical and growth signals, as well as organization of the actin-based cytoskeleton. However, two important membrane junctions maintain the cellular integrity of the myocardium: (1) cell–matrix adhesion sites, and (2) cell–cell junctions that reside in the intercalated disc (fascia adherens, desmosomes and gap junctions). Vcl-null embryonic fibroblasts display increased motility, invasiveness and resistance to apoptosis (Subauste et al., 2005; Subauste et al., 2004). Our work also describes that loss of Vcl is anti-apoptotic given that protein expression of cleaved PARP and cleaved caspase 3 were reduced after Vcl reduction (Fig. 7E,F). It has been shown that tethering of microtubule plus-ends at adherens junctions promotes the delivery of Cx hemichannels to the cell-to-cell border (Shaw et al., 2007). Furthermore, it has been shown that actin is a necessary component of the cytoskeletal-based forward trafficking apparatus for Cx43 (Smyth et al., 2012). The

actin cytoskeleton participates in the initial membrane remodeling stage when cells require an enhanced rate of autophagosome formation, and different members of the Rho family tightly regulate this actin function (Aguilera et al., 2012). Maintenance of cellular adhesions through structural glycoprotein binding to extracellular matrix is necessary for survival of cardiac myocytes. Anoïkis is defined as programmed cell death owing to loss of cell-to-matrix interactions (Michel, 2003). Weakened adhesion sites induce damage to the sarcolemma and might induce necrotic cell death, which can occur during anoïkis. Beating cardiac myocytes are extremely susceptible to membrane rupture. Our data here also suggest that Vcl reduction inhibits autophagic, as well as apoptotic, signaling compared to cells with physiological Vcl expression.

Study limitations

Ideally, our study would have studied Vcl in a myocyte model system where Vcl protein expression was essentially zero. Unfortunately, we found that even with reduction of Vcl to ~50% of normal physiological levels, profound biochemical and morphological changes resulted. It was important to investigate a population of healthy cells. We believe that our data clearly shows that physiological Vcl expression is necessary for cardiomyocyte integrity. A further limitation was that some of our study relied on use of neonatal cardiac myocytes, which are different from adult cells. We were not able to use Vcl-deficient adult cardiac myocytes (e.g. ones derived from our cVclKO mice) for biochemical analysis, because these cells are extremely fragile and intolerant to standard cell isolation techniques.

A limitation of our manuscript is that we cannot absolutely prove that loss of ZO-1–Vcl binding is the only mechanism responsible for perturbation of gap junction communication, all the changes in signal transduction or cardiac myocyte necrosis. To do so would require more precise localization of the Vcl–ZO-1 binding domain(s) and production of mutant Vcl and ZO-1 constructs that do not perturb any other function of Vcl and ZO-1. Ultimately these mutants could be used to replace the expression of the respective wild-type myocyte protein with the mutant one. Future work is required for this purpose.

Implications

The current study shows that diminished Vcl triggers a reduction in integrin as well as connexin-based cell adhesions, thereby contributing to the reduction of membrane integrity owing to weakened integrin and gap junctional attachment sites. These impaired contact sites might lead to diminished cardiac myocyte and heart function, and predispose the heart towards arrhythmias. A key role of gap junctional communication is rapid and coordinated action potential propagation, and therefore gap junctions are studied as new pharmacological targets to control cardiac arrhythmias (Colussi et al., 2011; O'Quinn et al., 2011). Recently, a role for Cx43 in intercellular cell adhesions and Na^+ channel function has been proposed (Agullo-Pascual and Delmar, 2012). Single-gene mutations of sarcomeric, metabolic, Z-disc-related and desmosomal proteins in humans have been linked to increased risk of developing heart failure (Morita et al., 2005). Genes currently known to be involved in familial cardiomyopathies also affect structural, cytoskeletal, Ca^{2+} cycling and mitochondrial proteins (Hershberger et al., 2009). One of these genes is Vcl and its splice-variant isoform MetaVcl (MVcl). Mutations in MVcl and Vcl are known to be associated with dilated as well as hypertrophic human cardiomyopathy (Olson et al., 2002; Vasile et al., 2006a; Vasile et al., 2006b; Vasile et al., 2006c). Furthermore, Vcl was found to be absent in cardiac tissue of a patient with dilated cardiomyopathy (Maeda et al., 1997). In addition, *Trypanosoma cruzi* infection can lead to cardiac dysfunction and arrhythmias. This is relevant because a significant reduction of Vcl expression at costameres, as well as irregular alignment of Vcl at intercalated discs has been observed after *Trypanosoma cruzi* infection (Melo et al., 2004). Recently, it has been shown that Vcl deficiency increased systolic stiffness, by increasing interfilament spacing, and thereby could induce mechanical stress in sarcomeres (Tangney et al., 2013). These reports all illustrate the role of Vcl as a cardiomyopathy-linked gene. Previous work using hemizygous VclKO mice has shown that these animals had altered intercalated disc structure and that they were intolerant to hemodynamic stress (Zemljic-Harpf et al., 2004). Our studies in cVclKO mice have shown that cardiomyocyte-specific Vcl reduction altered Cx43 expression, and induced either lethal arrhythmias or dilated cardiomyopathy (Zemljic-Harpf et al., 2007).

It should be noted that ZO-1 has been shown to be a key player in gap junction function and stabilization in several prior studies (Giepmans and Moolenaar, 1998; Hunter et al., 2005; Rhett and Gourdie, 2012; Rhett et al., 2011; Toyofuku et al., 1998). How ZO-1 is incorporated into the borders of the gap junctional plaque is not fully understood. However, it has been shown previously that ZO-1 can be localized to gap junctional border zones using a mechanism independent from its direct binding to the C-terminal residues in Cx43 (Hunter and Gourdie, 2008). Given that our current data shows that Vcl and ZO-1 directly interact, we suggest that Vcl might function as a linker anchoring ZO-1 to gap junctions, the actin cytoskeleton and even other common binding partners such as F-actin, α-actinin, and α-catenin. With this, we would suggest that the novel Vcl–ZO-1 interaction discussed here could be important in modulating the function of gap, adherens and tight junctions in many tissues.

Our data describe Vcl as an important new target to enhance and ensure proper gap junctional communication in cardiac myocytes. Gap junction expression is reduced in end-stage heart failure, and these hearts are prone to develop lethal arrhythmias. Therefore, as proposed by Basso and colleagues, understanding the molecular mechanisms of crosstalk from gap junctions to the actin cytoskeleton, ion channels and the nucleus is required to move from symptomatic to targeted therapy of heart failure (Basso et al., 2011). This would potentially enable both prevention of disease onset and also modification of its progression. More studies are needed to investigate whether Vcl could serve as a novel heart failure treatment target.

In summary, we demonstrate here for the first time that ZO-1 directly interacts with Vcl and that ZO-1, Vcl and Cx43 form a scaffolding complex in cardiac myocytes. Vcl excision in myocytes results in a reduction of the integral proteins β1D integrin and Cx43, as well as diminished expression of the membrane-associated proteins ZO-1, talin and tubulin. Vcl reduction in cardiac myocytes impairs gap junctional communication, reduces PI3K signaling, and activates Akt and ERK1/2. Our studies in cardiac myocytes suggest that reduced Vcl expression does not induce apoptotic cell death, and that Vcl-deficient cells are more likely to undergo cellular necrosis. These studies describe a novel role of Vcl in ensuring gap-junction-based intracellular signaling in cardiac myocytes compatible with its crucial role in both cardiac rhythm and function.

Journal of Cell Science (2014) 127, 1104–1116 doi:10.1242/jcs.143743

MATERIALS AND METHODS

Cardiac myocyte isolation and culture

The experimental procedures were conducted in accordance with the animal care guidelines, approved by the institutional animal care and use committee, and all mice were housed in an AALAC-approved facility. Adult cardiac myocytes were isolated from 2–3-month-old wild-type mice as previously described (Li et al., 2012; O'Connell et al., 2007). These cells were cultured for 4 h and either fixed with acetone for immunomicroscopic analyses or lysed for preparation of protein. Neonatal mouse cardiac myocytes (NMVMs) were isolated form 0–2-day-old $Vcl^{fl/fl}$ mouse hearts (Zemljic-Harpf et al., 2007). For culture, hearts were excised, the atria were removed and then the ventricular pieces were digested overnight in 50 ml of 0.5 mg/ml trypsin-HBSS at 4℃. On the following day, 25 ml of the trypsin solution was replaced by serum-free medium and digested for 3–4 minutes with gentle agitation (100–150 rpm). Subsequently the trypsin/serum free medium solution was removed and digestion was continued in type II collagenase (200–300 Units/ml, Worthington Biochemical Corporation, Lakewood, NJ) for three additional digestions, each for 5–7 min. Adding ice-cold serum-containing medium to inactivate collagenase-II terminated each collagenase digestion. Supernatants from digests were pooled and cells were collected by centrifugation. Two pre-plating steps, each for 1 h on uncoated tissue-culture dishes, were used to further purify NMVMs from this supernatant, because only non-myocyte cells rapidly adhere to these uncoated dishes. Approximately 5×10^6–6×10^6 cells were plated onto each 60-mm culture dish, which were coated with 0.2% gelatin/fibronectin (1 µg/ml; F0635, Sigma, St. Louis, MO) to generate confluent beating cultures. Cells were maintained in serum-containing medium (75% DMEM, 25% M-199, 10% fetal bovine serum and 5% horse serum). Only confluent cultures of NMVM were used.

Adenoviral infection of NMVM cultures

Five days after plating the $Vcl^{fl/fl}$ NMVMs, they were infected with recombinant adenovirus (AdV) expressing either Cre-recombinase or LacZ, at MOI=5 (Iwatate et al., 2003). Cells were cultured with the viral containing medium for 24 h, and then media replaced with serum-containing medium. Cultures were continued for periods as outlined in results, with new media replaced daily.

Immunofluorescence, immunoprecipitation and immunoblotting analyses

For immunofluorescence studies, cultured adult and NMVMs, as well as frozen cardiac tissue sections (5–7-µm thick) were fixed with ice-cold acetone for 7 min and washed with PBS. After blocking for 30 min at room temperature, cells or tissues were stained (overnight at 4℃) with commercially available antibodies [anti-Vcl (V9131, Sigma, St. Louis, MO), anti-Cx43 (C6219, Sigma), anti-ZO-1 (40-2300, Zymed/Invitrogen, Carlsbad, CA), anti-CD31 (PECAM-1) clone MEC 13.3 (553370, BD Biosciences, San Jose, CA), anti-α-actinin, EA53 (A7811, Sigma) and DAPI (Molecular Probes, Invitrogen, Carlsbad, CA)], as previously described (Zemljic-Harpf et al., 2004).

For immunoblotting, whole mouse heart tissue or cultured myocytes were lysed in buffer containing 50 mM Tris-HCl pH 7.5, 150 mM NaCl, 1 mM EDTA, 1% deoxycholic acid, 0.2% SDS, 1% NP-40, and equal protein amounts (5 µg for structural protein analysis, 50 µg for signaling proteins) were used for immunoblotting as previously described (Zemljic-Harpf et al., 2004). Membranes were blocked in 3% BSA for 30 min at room temperature and then incubated overnight at 4℃ with commercially available primary antibodies, as listed below, and visualized using chemiluminescent substrate for the detection of horseradish peroxidase (Pierce®, ECL Western Blotting Substrate). Densitometric quantitation was performed digitally (n=at least 3 per treatment, three replicates for each experiment). Statistical analysis was performed using un-paired Student's t-test ($P<0.05$ was considered significant). Data are displayed as mean±s.e.m.

For immunoprecipitations, total protein lysate (0.5 mg) was pre-cleared with protein-G–agarose (Roche Diagnostics, Indianapolis, IN) and then incubated with either anti-Vcl, anti-ZO-1, or anti-Cx43 antibodies (as listed below) for 2 h, followed by overnight incubation with protein-G–agarose at 4℃. Washes and immunoblotting was carried out as previously described (Pham et al., 2000).

Antibodies

The following primary antibodies were used (catalog numbers are given in parenthesis): Abcam, anti-β catenin (ab6302); Cell Signaling, anti-PI3K p85 (4292), anti-PTEN (9552), anti-total Akt (9272), anti-phosphoAkt$^{(Ser473)}$ (9271), anti-phosphoAkt$^{(Thr308)}$ (4056), anti-total p44/42 MAPK (ERK1/2) (9102), anti-phospho-p44/42 MAPK$^{(Tyr202/Tyr204)}$ (ERK1/2) (9106), anti-beclin (3738), anti-LC3B (2775), anti-cleaved PARP (9544), and anti-caspase 3 (9662); Santa Cruz Biotechnology, anti-GAPDH (sc-25778), anti-RhoA (26C4) (sc-418); Sigma, anti-Vcl (V9131), anti-Cx43 (C6219), anti-α-actinin (A7811), anti-tubulin (T5168), and anti-talin (T3287); and Zymed, anti-ZO-1 (40–2300). The polyclonal rabbit anti-β1D integrin antibody was used as previously described (Pham et al., 2000).

Yeast two-hybrid screening

Yeast two-hybrid and β-galactosidase assays were performed using the Matchmaker GAL4 Two-hybrid Mating System (Clontech, Palo Alto, CA). To assay for the interaction between Vcl and ZO-1, coding sequences for full-length (0–3.2 kb) and deletion mutants (0–2.5 kb and 1.6–3.2 kb) of Vcl were generated by PCR and subcloned into the pGBKT7 bait vector. Coding sequences for deletion mutants of ZO-1 (0–2.5 kb, 0–1.5 kb and 1.5–2.5 kb) were generated by PCR and subcloned into the target vector pGADT7. PCR primers used for construction of all fragments are displayed in supplementary material Table S1. Sequences were confirmed using standard technology. Baits were transformed into the yeast strain AH109 and mated overnight with Y187 yeasts pre-transformed with ZO-1 targets. Mating cultures were assayed for growth on selection plates lacking the amino acids leucine and tryptophan (SD −LW). Two independent positive mating colonies per each protein–protein interaction were assessed for β-galactosidase activity using the ortho-nitrophenyl-β-d-galactopyranoside (ONPG)-driven liquid culture method as described by the manufacturer. A well-known interaction between murine p53 and SV40 T-antigen TD1, and unlikely interactions between TD1 or p53 against ZO-1 and Vcl were used as positive and negative controls, respectively (Ali and DeCaprio, 2001).

In a second set of experiments, the Matchmaker GAL4 Two-hybrid Mating System (Clontech, Palo Alto, CA) was used to confirm the interaction between Vcl and ZO-1, and to screen for a minimal interacting domain in ZO-1 using the same system (Fig. 3B,C). Primers and templates for PCR are described in supplementary material Table S1.

Cytotoxicity assay

Lactate dehydrogenase release was measured in neonatal cardiac myocyte cell culture supernatants using a colorimetric assay kit according to the manufacturer's instructions (catalog number 04744926001, Roche Applied Science, Indianapolis, IN).

Dye transfer and scrape loading for the assessment of gap junction communication

For dye transfer studies, NMVMs were plated on acid-etched glass coverslips that were pre-coated with a mixture of 0.2% gelatin and fibronectin (1 µg/ml, Sigma, F0635). They were then infected with various recombinant adenoviruses as discussed above. Using a patch pipette electrode in the whole-cell mode, individual cardiac myocytes were injected with PBS (17-516, Lonza Walkersville, MD) containing a combination of 1 mM each Lucifer Yellow and Rhodamine dextran (L453 and D1817 respectively, Sigma-Aldrich/Invitrogen, St. Louis, MO). Images were taken 25 min after dye injection and analyzed as previously described (Makino et al., 2008; Valiunas et al., 2002).

For scrape loading studies, NMVMs were prepared and infected identically to in the dye transfer studies. The culture medium was removed and saved. Cells were washed three times with 37℃ PBS without Mg^{2+} and Ca^{2+} (17-516, Lonza,). Then, a razor blade was used to

generate a longitudinal scratch though the confluent monolayer. Cells were immediately loaded with PBS containing 1 mM Lucifer Yellow and 1 mM Rhodamine dextran dyes for 2 min by flooding the scratch. They were then rinsed three times with PBS, and incubated for an additional 20 min in the culture medium saved prior to dye loading. Dye transfer was then assessed by image acquisition 25 min after dye loading, and analyzed as previously described (Boswell et al., 2009; el-Fouly et al., 1987; Li et al., 2011; Opsahl and Rivedal, 2000).

Acknowledgements
We thank Valeria Mezzano (NYU School of Medicine, New York, NY) and Farah Sheikh (UCSD School of Medicine, La Jolla, CA) for helpful discussions and technical advice in optimizing the neonatal myocyte isolation protocol. We further acknowledge Jason Yuan (U. Illinois-Chicago, Chicago, IL.) and Martin Marsala (UCSD School of Medicine, La Jolla, CA) for their scientific support.

Competing interests
The authors declare no competing interests.

Author contributions
A.E.Z.-H was responsible for the execution and design of most of the experiments, drafting and revision of the manuscript and figures. J.C.G. contributed to the execution of tissue culture and immunoblotting studies, and provided manuscript revision. O. P. acquired Rhodamine Dextran and Lucifer Yellow microinjection data, and provided manuscript revision. E.K.A. maintained and genotyped mouse colonies, and performed cryosectioning. A.R.B. generated the diagrammatic representation in figure 8 together with A.E.Z.-H and R.S.R. A.A.D. designed and carried out yeast two-hybrid studies, and provided manuscript revision. R.S.R. was responsible for guiding overall research direction, contributed to the experimental design, writing the manuscript and to final figure composition.

Funding
This work was supported by the National Institutes of Health [grant numbers PO1 HL 46345, RO1 HL088390 and RO1 HL103566 to R.S.R.]; and the American Heart Association [grant number AHA-BGIA 2260359 to A.E.Z.-H.]. Deposited in PMC for release after 12 months.

Supplementary material
Supplementary material available online at
http://jcs.biologists.org/lookup/suppl/doi:10.1242/jcs.143743/-/DC1

References
Aguilera, M. O., Berón, W. and Colombo, M. I. (2012). The actin cytoskeleton participates in the early events of autophagosome formation upon starvation induced autophagy. *Autophagy* **8**, 1590-1603.
Agullo-Pascual, E. and Delmar, M. (2012). The noncanonical functions of Cx43 in the heart. *J. Membr. Biol.* **245**, 477-482.
Ali, S. H. and DeCaprio, J. A. (2001). Cellular transformation by SV40 large T antigen: interaction with host proteins. *Semin. Cancer Biol.* **11**, 15-23.
Basso, C., Bauce, B., Corrado, D. and Thiene, G. (2011). Pathophysiology of arrhythmogenic cardiomyopathy. *Nat. Rev. Cardiol.* **9**, 223-233.
Bois, P. R., O'Hara, B. P., Nietlispach, D., Kirkpatrick, J. and Izard, T. (2006). The vinculin binding sites of talin and alpha-actinin are sufficient to activate vinculin. *J. Biol. Chem.* **281**, 7228-7236.
Borgon, R. A., Vonrhein, C., Bricogne, G., Bois, P. R. and Izard, T. (2004). Crystal structure of human vinculin. *Structure* **12**, 1189-1197.
Boswell, B. A., Le, A. C. and Musil, L. S. (2009). Upregulation and maintenance of gap junctional communication in lens cells. *Exp. Eye Res.* **88**, 919-927.
Chandrasekar, I., Stradal, T. E., Holt, M. R., Entschladen, F., Jockusch, B. M. and Ziegler, W. H. (2005). Vinculin acts as a sensor in lipid regulation of adhesion-site turnover. *J. Cell Sci.* **118**, 1461-1472.
Chetram, M. A. & Hinton, C. V. (2012). PTEN regulation of ERK1/2 signaling in cancer. *J Recept Signal Transduct Res* **32(4)**, 190-195.
Ching, J. K., Rajguru, P., Marupudi, N., Banerjee, S. and Fisher, J. S. (2010). A role for AMPK in increased insulin action after serum starvation. *Am. J. Physiol.* **299**, C1171-C1179.
Colussi, C., Rosati, J., Straino, S., Spallotta, F., Berni, R., Stilli, D., Rossi, S., Musso, E., Macchi, E., Mai, A. et al. (2011). Nε-lysine acetylation determines dissociation from GAP junctions and lateralization of connexin 43 in normal and dystrophic heart. *Proc. Natl. Acad. Sci. USA* **108**, 2795-2800.
Costa, C. and Hirsch, E. (2010). More than just kinases: the scaffolding function of PI3K. *Curr. Top. Microbiol. Immunol.* **346**, 171-181.
Craig, S. W. and Pardo, J. V. (1983). Gamma actin, spectrin, and intermediate filament proteins colocalize with vinculin at costameres, myofibril-to-sarcolemma attachment sites. *Cell Motil.* **3**, 449-462.
Decrock, E., Vinken, M., De Vuyst, E., Krysko, D. V., D'Herde, K., Vanhaecke, T., Vandenabeele, P., Rogiers, V. and Leybaert, L. (2009). Connexin-related signaling in cell death: to live or let die? *Cell Death Differ.* **16**, 524-536.
Delmar, M. and Liang, F. X. (2012). Connexin43 and the regulation of intercalated disc function. *Heart Rhythm* **9**, 835-838.
Di Paolo, G. and De Camilli, P. (2006). Phosphoinositides in cell regulation and membrane dynamics. *Nature* **443**, 651-657.
Dumbauld, D. W., Lee, T. T., Singh, A., Scrimgeour, J., Gersbach, C. A., Zamir, E. A., Fu, J., Chen, C. S., Curtis, J. E., Craig, S. W. et al. (2013). How vinculin regulates force transmission. *Proc. Natl. Acad. Sci. USA* **110**, 9788-9793.
El-Fouly, M. H., Trosko, J. E. and Chang, C. C. (1987). Scrape-loading and dye transfer. A rapid and simple technique to study gap junctional intercellular communication. *Exp. Cell Res.* **168**, 422-430.
Fanning, A. S. and Anderson, J. M. (2009). Zonula occludens-1 and -2 are cytosolic scaffolds that regulate the assembly of cellular junctions. *Ann. N. Y. Acad. Sci.* **1165**, 113-120.
Fanning, A. S., Ma, T. Y. and Anderson, J. M. (2002). Isolation and functional characterization of the actin binding region in the tight junction protein ZO-1. *FASEB J.* **16**, 1835-1837.
Ghigo, A., Morello, F., Perino, A. and Hirsch, E. (2012). Phosphoinositide 3-kinases in health and disease. *Subcell. Biochem.* **58**, 183-213.
Giepmans, B. N. and Moolenaar, W. H. (1998). The gap junction protein connexin43 interacts with the second PDZ domain of the zona occludens-1 protein. *Curr. Biol.* **8**, 931-934.
Gilmore, A. P. and Burridge, K. (1996). Regulation of vinculin binding to talin and actin by phosphatidyl-inositol-4-5-bisphosphate. *Nature* **381**, 531-535.
Grashoff, C., Hoffman, B. D., Brenner, M. D., Zhou, R., Parsons, M., Yang, M. T., McLean, M. A., Sligar, S. G., Chen, C. S., Ha, T. et al. (2010). Measuring mechanical tension across vinculin reveals regulation of focal adhesion dynamics. *Nature* **466**, 263-266.
Hershberger, R. E., Lindenfeld, J., Mestroni, L., Seidman, C. E., Taylor, M. R., Towbin, J. A.; Heart Failure Society of America (2009). Genetic evaluation of cardiomyopathy – a Heart Failure Society of America practice guideline. *J. Card. Fail.* **15**, 83-97.
Hu, K., Ji, L., Applegate, K. T., Danuser, G. and Waterman-Storer, C. M. (2007). Differential transmission of actin motion within focal adhesions. *Science* **315**, 111-115.
Hunter, A. W. and Gourdie, R. G. (2008). The second PDZ domain of zonula occludens-1 is dispensable for targeting to connexin 43 gap junctions. *Cell Commun. Adhes.* **15**, 55-63.
Hunter, A. W., Barker, R. J., Zhu, C. and Gourdie, R. G. (2005). Zonula occludens-1 alters connexin43 gap junction size and organization by influencing channel accretion. *Mol. Biol. Cell* **16**, 5686-5698.
Inoko, A., Itoh, M., Tamura, A., Matsuda, M., Furuse, M. and Tsukita, S. (2003). Expression and distribution of ZO-3, a tight junction MAGUK protein, in mouse tissues. *Genes Cells* **8**, 837-845.
Ishikawa, S., Kuno, A., Tanno, M., Miki, T., Kouzu, H., Itoh, T. and Miura, T. (2012). Role of connexin-43 in protective PI3K-Akt-GSK-3beta signaling in cardiomyocytes. *Am J Physiol Heart Circ Physiol* **302(12)**, H2536-2544.
Iwatate, M., Gu, Y., Dieterle, T., Iwanaga, Y., Peterson, K. L., Hoshijima, M., Chien, K. R. and Ross, J. (2003). In vivo high-efficiency transcoronary gene delivery and Cre-LoxP gene switching in the adult mouse heart. *Gene Ther.* **10**, 1814-1820.
Izard, T., Evans, G., Borgon, R. A., Rush, C. L., Bricogne, G. and Bois, P. R. (2004). Vinculin activation by talin through helical bundle conversion. *Nature* **427**, 171-175.
Jesaitis, L. A. and Goodenough, D. A. (1994). Molecular characterization and tissue distribution of ZO-2, a tight junction protein homologous to ZO-1 and the Drosophila discs-large tumor suppressor protein. *J. Cell Biol.* **124**, 949-961.
Kardami, E., Dang, X., Iacobas, D. A., Nickel, B. E., Jeyaraman, M., Srisakuldee, W., Makazan, J., Tanguy, S. and Spray, D. C. (2007). The role of connexins in controlling cell growth and gene expression. *Prog. Biophys. Mol. Biol.* **94**, 245-264.
Katso, R., Okkenhaug, K., Ahmadi, K., White, S., Timms, J. and Waterfield, M. D. (2001). Cellular function of phosphoinositide 3-kinases: implications for development, homeostasis, and cancer. *Annu Rev Cell Dev Biol* **17**, 615-675.
Katsuno, T., Umeda, K., Matsui, T., Hata, M., Tamura, A., Itoh, M., Takeuchi, K., Fujimori, T., Nabeshima, Y., Noda, T. et al. (2008). Deficiency of zonula occludens-1 causes embryonic lethal phenotype associated with defected yolk sac angiogenesis and apoptosis of embryonic cells. *Mol. Biol. Cell* **19**, 2465-2475.
Kerr, B. A., Ma, L., West, X. Z., Ding, L., Malinin, N. L., Weber, M. E. and Byzova, T. V. (2013). Interference with akt signaling protects against myocardial infarction and death by limiting the consequences of oxidative stress. *Sci Signal* **6(287)**, ra67. doi: 6/287/ra67
Kostin, S., Hein, S., Arnon, E., Scholz, D. and Schaper, J. (2000). The cytoskeleton and related proteins in the human failing heart. *Heart Fail. Rev.* **5**, 271-280.
Li, M. W., Mruk, D. D., Lee, W. M. and Cheng, C. Y. (2009). Connexin 43 and plakophilin-2 as a protein complex that regulates blood-testis barrier dynamics. *Proc. Natl. Acad. Sci. USA* **106**, 10213-10218.
Li, K., Yao, J., Shi, L., Sawada, N., Chi, Y., Yan, Q., Matsue, H., Kitamura, M. and Takeda, M. (2011). Reciprocal regulation between proinflammatory cytokine-induced inducible NO synthase (iNOS) and connexin43 in bladder smooth muscle cells. *J. Biol. Chem.* **286**, 41552-41562.

Li, R., Wu, Y., Manso, A. M., Gu, Y., Liao, P., Israeli, S., Yajima, T., Nguyen, U., Huang, M. S., Dalton, N. D. et al. (2012). β1 integrin gene excision in the adult murine cardiac myocyte causes defective mechanical and signaling responses. *Am. J. Pathol.* **180**, 952-962.

Lin, R. C., Weeks, K. L., Gao, X. M., Williams, R. B., Bernardo, B. C., Kiriazis, H. and McMullen, J. R. (2010). PI3K(p110 alpha) protects against myocardial infarction-induced heart failure: identification of PI3K-regulated miRNA and mRNA. *Arterioscler Thromb Vasc Biol* **30(4)**, 724-732. doi: 30/4/724

Maeda, M., Holder, E., Lowes, B., Valent, S. and Bies, R. D. (1997). Dilated cardiomyopathy associated with deficiency of the cytoskeletal protein metavinculin. *Circulation* **95**, 17-20.

Maiers, J. L., Peng, X., Fanning, A. S. and DeMali, K. A. (2013). ZO-1 recruitment to α-catenin—a novel mechanism for coupling the assembly of tight junctions to adherens junctions. *J. Cell Sci.* **126**, 3904-3915.

Makino, A., Platoshyn, O., Suarez, J., Yuan, J. X. and Dillmann, W. H. (2008). Downregulation of connexin40 is associated with coronary endothelial cell dysfunction in streptozotocin-induced diabetic mice. *Am. J. Physiol.* **295**, C221-C230.

McMullen, J. R., Amirahmadi, F., Woodcock, E. A., Schinke-Braun, M., Bouwman, R. D., Hewitt, K. A. and Jennings, G. L. (2007). Protective effects of exercise and phosphoinositide 3-kinase(p110alpha) signaling in dilated and hypertrophic cardiomyopathy. *Proc Natl Acad Sci U S A,* **104(2)**, 612-617.

Melo, T. G., Almeida, D. S., de Meirelles, M. N. and Pereira, M. C. (2004). Trypanosoma cruzi infection disrupts vinculin costameres in cardiomyocytes. *Eur. J. Cell Biol.* **83**, 531-540.

Michel, J. B. (2003). Anoikis in the cardiovascular system: known and unknown extracellular mediators. *Arterioscler. Thromb. Vasc. Biol.* **23**, 2146-2154.

Morita, H., Seidman, J. and Seidman, C. E. (2005). Genetic causes of human heart failure. *J. Clin. Invest.* **115**, 518-526.

Müller, S. L., Portwich, M., Schmidt, A., Utepbergenov, D. I., Huber, O., Blasig, I. E. and Krause, G. (2005). The tight junction protein occludin and the adherens junction protein alpha-catenin share a common interaction mechanism with ZO-1. *J. Biol. Chem.* **280**, 3747-3756.

Niggli, V. and Gimona, M. (1993). Evidence for a ternary interaction between alpha-actinin, (meta)vinculin and acidic-phospholipid bilayers. *Eur. J. Biochem.* **213**, 1009-1015.

Niggli, V., Dimitrov, D. P., Brunner, J. and Burger, M. M. (1986). Interaction of the cytoskeletal component vinculin with bilayer structures analyzed with a photoactivatable phospholipid. *J. Biol. Chem.* **261**, 6912-6918.

O'Connell, T. D., Rodrigo, M. C. and Simpson, P. C. (2007). Isolation and culture of adult mouse cardiac myocytes. *Methods Mol. Biol.* **357**, 271-296.

O'Quinn, M. P., Palatinus, J. A., Harris, B. S., Hewett, K. W. and Gourdie, R. G. (2011). A peptide mimetic of the connexin43 carboxyl terminus reduces gap junction remodeling and induced arrhythmia following ventricular injury. *Circ. Res.* **108**, 704-715.

Olson, T. M., Illenberger, S., Kishimoto, N. Y., Huttelmaier, S., Keating, M. T. and Jockusch, B. M. (2002). Metavinculin mutations alter actin interaction in dilated cardiomyopathy. *Circulation* **105**, 431-437.

Opsahl, H. and Rivedal, E. (2000). Quantitative determination of gap junction intercellular communication by scrape loading and image analysis. *Cell Adhes. Commun.* **7**, 367-375.

Palmer, S. M., Playford, M. P., Craig, S. W., Schaller, M. D. and Campbell, S. L. (2009). Lipid binding to the tail domain of vinculin: specificity and the role of the N and C termini. *J. Biol. Chem.* **284**, 7223-7231.

Pardo, J. V., Siliciano, J. D. and Craig, S. W. (1983). A vinculin-containing cortical lattice in skeletal muscle: transverse lattice elements ("costameres") mark sites of attachment between myofibrils and sarcolemma. *Proc. Natl. Acad. Sci. USA* **80**, 1008-1012.

Peng, X., Cuff, L. E., Lawton, C. D. and DeMali, K. A. (2010). Vinculin regulates cell-surface E-cadherin expression by binding to beta-catenin. *J. Cell Sci.* **123**, 567-577.

Pham, C. G., Harpf, A. E., Keller, R. S., Vu, H. T., Shai, S. Y., Loftus, J. C. and Ross, R. S. (2000). Striated muscle-specific beta(1D)-integrin and FAK are involved in cardiac myocyte hypertrophic response pathway. *Am. J. Physiol.* **279**, H2916-H2926.

Rhett, J. M. and Gourdie, R. G. (2012). The perinexus: a new feature of Cx43 gap junction organization. *Heart Rhythm* **9**, 619-623.

Rhett, J. M., Jourdan, J. and Gourdie, R. G. (2011). Connexin 43 connexon to gap junction transition is regulated by zonula occludens-1. *Mol. Biol. Cell* **22**, 1516-1528.

Saffitz, J. E., Laing, J. G. and Yamada, K. A. (2000). Connexin expression and turnover : implications for cardiac excitability. *Circ. Res.* **86**, 723-728.

Saunders, R. M., Holt, M. R., Jennings, L., Sutton, D. H., Barsukov, I. L., Bobkov, A. and Critchley, D. R. (2006). Role of vinculin in regulating focal adhesion turnover. *Eur J Cell Biol* **85 (6)**, 487-500. doi: S0171-9335(06)00025-2

Shaw, R. M., Fay, A. J., Puthenveedu, M. A., von Zastrow, M., Jan, Y. N. and Jan, L. Y. (2007). Microtubule plus-end-tracking proteins target gap junctions directly from the cell interior to adherens junctions. *Cell* **128**, 547-560.

Shiraishi, I., Simpson, D. G., Carver, W., Price, R., Hirozane, T., Terracio, L. and Borg, T. K. (1997). Vinculin is an essential component for normal myofibrillar arrangement in fetal mouse cardiac myocytes. *J. Mol. Cell. Cardiol.* **29**, 2041-2052.

Smyth, J. W., Vogan, J. M., Buch, P. J., Zhang, S. S., Fong, T. S., Hong, T. T. and Shaw, R. M. (2012). Actin cytoskeleton rest stops regulate anterograde traffic of connexin 43 vesicles to the plasma membrane. *Circ. Res.* **110**, 978-989.

Song, L. S., Guatimosim, S., Gomez-Viquez, L., Sobie, E. A., Ziman, A., Hartmann, H. and Lederer, W. J. (2005). Calcium biology of the transverse tubules in heart. *Ann N Y Acad Sci* **1047**, 99-111. doi: 1047/1/99

Subauste, M. C., Pertz, O., Adamson, E. D., Turner, C. E., Junger, S. and Hahn, K. M. (2004). Vinculin modulation of paxillin-FAK interactions regulates ERK to control survival and motility. *J. Cell Biol.* **165**, 371-381.

Subauste, M. C., Nalbant, P., Adamson, E. D. and Hahn, K. M. (2005). Vinculin controls PTEN protein level by maintaining the interaction of the adherens junction protein beta-catenin with the scaffolding protein MAGI-2. *J. Biol. Chem.* **280**, 5676-5681.

Tangney, J. R., Chuang, J. S., Janssen, M. S., Krishnamurthy, A., Liao, P., Hoshijima, M., Wu, X., Meininger, G. A., Muthuchamy, M., Zemljic-Harpf, A. et al. (2013). Novel role for vinculin in ventricular myocyte mechanics and dysfunction. *Biophys. J.* **104**, 1623-1633.

Tirziu, D., Giordano, F. J. and Simons, M. (2010). Cell communications in the heart. *Circulation* **122**, 928-937.

Toyofuku, T., Yabuki, M., Otsu, K., Kuzuya, T., Hori, M. and Tada, M. (1998). Direct association of the gap junction protein connexin-43 with ZO-1 in cardiac myocytes. *J. Biol. Chem.* **273**, 12725-12731.

Valiunas, V., Beyer, E. C. and Brink, P. R. (2002). Cardiac gap junction channels show quantitative differences in selectivity. *Circ. Res.* **91**, 104-111.

Vasile, V. C., Edwards, W. D., Ommen, S. R. and Ackerman, M. J. (2006a). Obstructive hypertrophic cardiomyopathy is associated with reduced expression of vinculin in the intercalated disc. *Biochem. Biophys. Res. Commun.* **349**, 709-715.

Vasile, V. C., Ommen, S. R., Edwards, W. D. and Ackerman, M. J. (2006b). A missense mutation in a ubiquitously expressed protein, vinculin, confers susceptibility to hypertrophic cardiomyopathy. *Biochem. Biophys. Res. Commun.* **345**, 998-1003.

Vasile, V. C., Will, M. L., Ommen, S. R., Edwards, W. D., Olson, T. M. and Ackerman, M. J. (2006c). Identification of a metavinculin missense mutation, R975W, associated with both hypertrophic and dilated cardiomyopathy. *Mol. Genet. Metab.* **87**, 169-174.

Weekes, J., Barry, S. T. and Critchley, D. R. (1996). Acidic phospholipids inhibit the intramolecular association between the N- and C-terminal regions of vinculin, exposing actin-binding and protein kinase C phosphorylation sites. *Biochem. J.* **314**, 827-832.

Weeks, K. L., Gao, X., Du, X. J., Boey, E. J. and Matsumoto, A, Bernardo, B. C. and McMullen, J. R. (2012). Phosphoinositide 3-kinase p110alpha is a master regulator of exercise-induced cardioprotection and PI3K gene therapy rescues cardiac dysfunction. *Circ Heart Fail* **5(4)**, 523-534. doi: CIRCHEARTFAILURE.112.966622

Weiss, E. E., Kroemker, M., Rüdiger, A. H., Jockusch, B. M. and Rüdiger, M. (1998). Vinculin is part of the cadherin-catenin junctional complex: complex formation between alpha-catenin and vinculin. *J. Cell Biol.* **141**, 755-764.

Wu, J., Li, J., Hu, H., Liu, P., Fang, Y. and Wu, D. (2012). Rho-Kinase Inhibitor, Fasudil, Prevents Neuronal Apoptosis via the Akt Activation and PTEN Inactivation in the Ischemic Penumbra of Rat Brain. *Cell Mol Neurobiol.*

Xu, W., Baribault, H. and Adamson, E. D. (1998). Vinculin knockout results in heart and brain defects during embryonic development. *Development* **125**, 327-337.

Yin, H. L. and Janmey, P. A. (2003). Phosphoinositide regulation of the actin cytoskeleton. *Annu. Rev. Physiol.* **65**, 761-789.

Zemljic-Harpf, A. E., Ponrartana, S., Avalos, R. T., Jordan, M. C., Roos, K. P., Dalton, N. D., Phan, V. Q., Adamson, E. D. and Ross, R. S. (2004). Heterozygous inactivation of the vinculin gene predisposes to stress-induced cardiomyopathy. *Am. J. Pathol.* **165**, 1033-1044.

Zemljic-Harpf, A. E., Miller, J. C., Henderson, S. A., Wright, A. T., Manso, A. M., Elsherif, L., Dalton, N. D., Thor, A. K., Perkins, G. A., McCulloch, A. D. et al. (2007). Cardiac-myocyte-specific excision of the vinculin gene disrupts cellular junctions, causing sudden death or dilated cardiomyopathy. *Mol. Cell. Biol.* **27**, 7522-7537.

Ziegler, W. H., Liddington, R. C. and Critchley, D. R. (2006). The structure and regulation of vinculin. *Trends Cell Biol.* **16**, 453-460.

Journal of Cell Science